Volume 7
Number 8
August 2020
Pages 1923–2172

Materials Horizons

rsc.li/materials-horizons

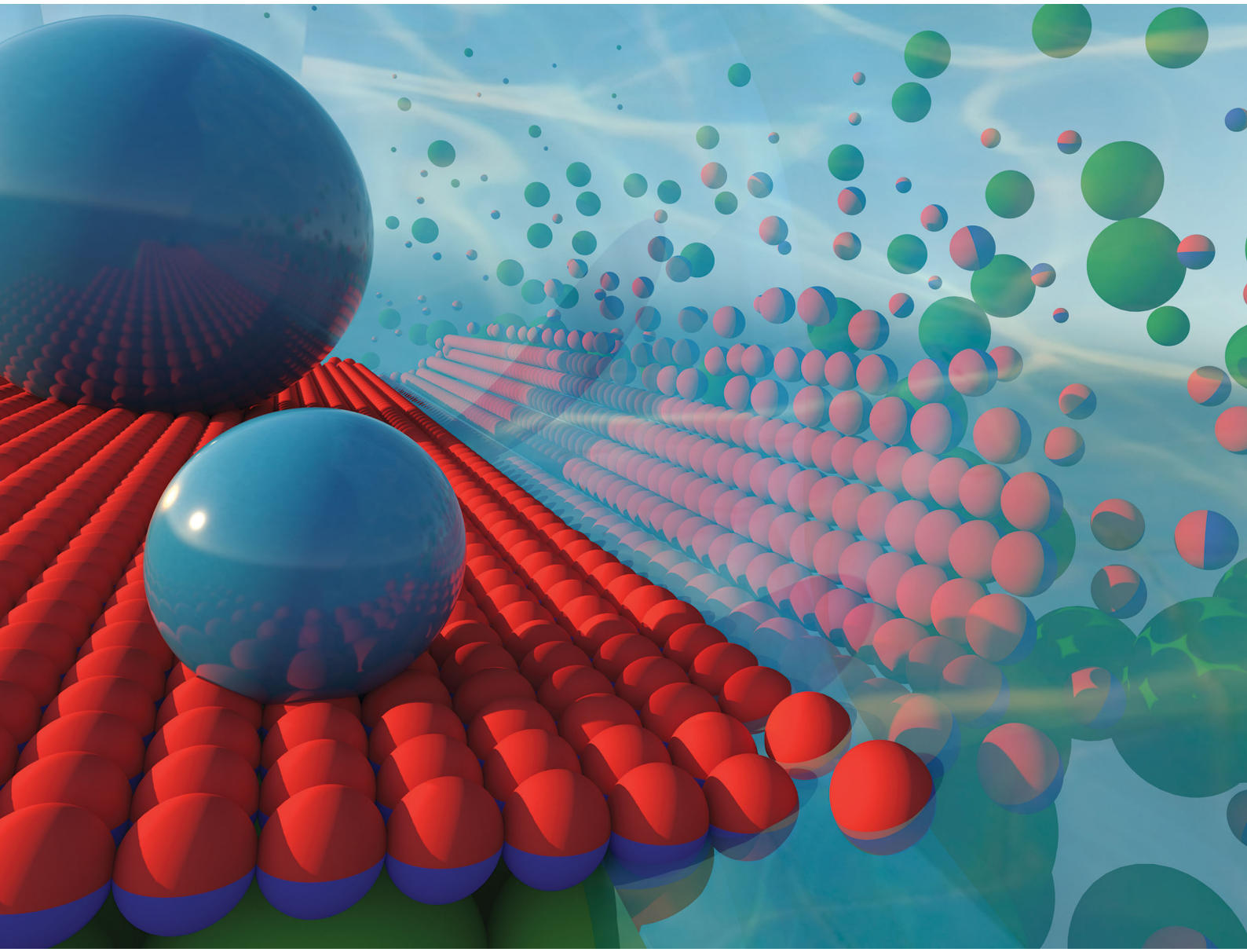

ISSN 2051-6347

ROYAL SOCIETY OF CHEMISTRY

COMMUNICATION
Shan Jiang *et al.*
Self-stratification of amphiphilic Janus particles at coating surfaces

Materials Horizons

ROYAL SOCIETY OF CHEMISTRY

COMMUNICATION

View Article Online
View Journal | View Issue

Check for updates

Cite this: *Mater. Horiz.*, 2020, 7, 2047

Received 8th April 2020,
Accepted 15th June 2020

DOI: 10.1039/d0mh00589d

rsc.li/materials-horizons

Self-stratification of amphiphilic Janus particles at coating surfaces†

Yifan Li,[a] Fei Liu,[a] Shensheng Chen,[b] Ayuna Tsyrenova,[a] Kyle Miller,[a] Emily Olson,[a] Rebecca Mort,[a] Devin Palm,[a] Chunhui Xiang,[c] Xin Yong[b] and Shan Jiang*[ad]

Amphiphilic Janus particles are mixed with homogeneous binder particles with strong adhesion to create robust hydrophobic coatings through a unique self-stratification process. Intriguingly, Janus particles form a complete and densely packed monolayer with their hydrophobic sides orienting towards air, which effectively increases the water contact angle to ~130°, while the hydrophilic sides sustain strong adhesion with the coating layer. The coating maintains its high contact angle even after solvent rinsing, whereas conventional coating completely breaks down. Experimental data and preliminary theoretical modeling suggest that the stratification are partially due to the strong adsorption of Janus particles at the water–air interface, although the detailed mechanisms require more thorough investigation. Remarkably, simply adding Janus particles renders a hydrophilic commercial primer coating surface hydrophobic and drastically reduces the surface tackiness. This cost-effective and commercially scalable method offers a convenient way to fabricate advanced structures at the interface and can be broadly applicable to many other colloidal systems.

New concepts

We discovered the unique self-stratification behaviours of Janus particles and successfully created durable hydrophobic coatings by adding Janus particles to binder polymers, including a common commercial primer product. Contrasting with homogeneous particle mixtures where stratification is driven passively by evaporation, Janus particles vigorously accumulate at the air–water interface in fast kinetics, with their hydrophobic sides orienting towards air. Since the hydrophilic side of Janus particles adheres strongly to the binder particles, this new system addresses the weak adhesion issue of conventional hydrophobic coatings. This new method offers cost-effective and commercially scalable solutions to many long-standing challenges in waterborne emulsion coatings, including water resistance, adhesion, surface hardness and film formation. The study also opens new fronts for Janus particle research and provides a novel strategy to self-assemble and fabricate hierarchical structures, which may find broad applications beyond coating materials, including cosmetics, adhesives, drug formulations and 3d printing.

Introduction

The revolutionary replacement of organic solvent-based coatings by waterborne emulsion latex polymer coatings has substantially reduced the prevalence of volatile organic compounds (VOCs), from 700 g L^{-1} in 1940s to ~50 g L^{-1} in 2010s.[1] The technology has generated profound impact in industry and everyday life, producing great environmental and health benefits. However, these waterborne coatings have created unique challenges in maintaining high coating performance, such as suspension stability, water resistance, film formation, and surface hardness. Many of the coating properties can hardly be achieved simultaneously with a simple system. For example, coating stability of waterborne latex paint requires emulsion particles to be hydrophilic and completely dispersible in water. However, upon drying, a water-resistant and hydrophobic coating film is preferable. A durable coating film demands excellent adhesion on the substrate surface, while showing good hardness (low tackiness) at the coating–air interface. This means it is beneficial to possess different or even opposite properties on the two sides of the coating films.

One approach to combine these different properties is to apply multiple coats. It is common practice to coat primers as the first layer to provide good adhesion.[2,3] After the primer is dried, a topcoat is then applied to afford more desirable surface properties. However, this approach consumes extra materials, time, and effort. For applications that require both performance and fast turn-around, such as traffic coating, a simple one coat solution is strongly preferred.[4] Another grand challenge in waterborne coating materials is to eliminate VOCs and create the "zero-VOC" paint.[5] Such coatings will further benefit environmental and

[a] Department of Materials Science and Engineering, Iowa State University of Science and Technology, Ames, IA 50011, USA. E-mail: sjiang1@iastate.edu
[b] Department of Mechanical Engineering, Binghamton University, Binghamton, NY 13902, USA
[c] Department of Apparel, Events and Hospitality Management, Iowa State University of Science and Technology, Ames, IA 50011, USA
[d] Division of Materials Science & Engineering, Ames National Laboratory, Ames, IA 50011, USA

† Electronic supplementary information (ESI) available. See DOI: 10.1039/d0mh00589d

Open Access Article. Published on 15 June 2020. Downloaded on 7/23/2025 4:24:04 PM.
This article is licensed under a Creative Commons Attribution-NonCommercial 3.0 Unported Licence.

Open Access Article. Published on 15 June 2020. Downloaded on 7/23/2025 4:24:04 PM.
This article is licensed under a Creative Commons Attribution-NonCommercial 3.0 Unported Licence.

consumer health. However, removing all the VOCs will make it difficult for latex particles to form an integral coating film unless the glass transition temperature (T_g) for polymer binder is greatly reduced. This can be done by altering the polymer chemistry or adding non-evaporative coalescent molecules, however doing so will inevitably hurt coating hardness and many other properties. Therefore, technology that can guarantee film formation while providing a hard coating surface becomes a holy grail in coating research. Most of the ideas have been developed around two-component "2K" systems and crosslinking chemistry, which usually are much more costly and require complicated chemistry and formulation.[6,7]

One innovative idea to address all these challenges is to develop one-pot, self-stratifying coating systems, where the surface of the coating film differs from the bulk. In this way, many coating properties dictated by the surface layer, such as tackiness, hardness, water resistance, and dirt pick-up, can be designed and optimized separately from the bulk materials.[8–12] However, conventional coating systems do not self-stratify. Previous studies demonstrated that self-stratification will only happen for polymers of specific chemistry or particle mixtures of certain size ratios when a coating suspension dries.[13–18] These constraints severely limit the application of self-stratification in common coating materials. In order to achieve effective stratification, current coating formulation and binder chemistry need to be comprehensively altered, which demands significant efforts.

Here we propose a new concept of self-stratification by using amphiphilic Janus particles, where one side of the particle is hydrophobic, and the other side is hydrophilic. It has been well-established that Janus particles can be viewed as colloidal surfactants that adsorb strongly at the interface.[19–21] The adsorption energy, defined as the interfacial energy change when a single particle moves from bulk phase to the interface, is directly related to the Janus particle geometry.[22,23] Janus particles with the perfect 50–50 (hydrophobic–hydrophilic) geometry has the highest amphiphilicity that leads to the highest adsorption energy. The theoretical calculation also suggests that the more Janus geometry deviates from 50–50, the less is the adsorption energy.[24]

Conventional self-stratification for homogeneous particle mixtures is driven passively by the drying of the solvent. The difference in diffusion rate for particles of different sizes will lead to a different amount of accumulation at the drying front.[25–29] The Peclet number, the ratio of the evaporation rate against the diffusion rate, is often used to quantify and predict the stratification behaviour. However, the Peclet number does not consider the surface adsorption of particles at all. For this reason, the self-stratification of amphiphilic Janus particles is more active due to their strong surface adsorption and the physics is completely different compared with conventional homogeneous particles.[30] Currently, no theory can be used to explain the active self-stratification of Janus particles. Our study provides experimental evidence and preliminary theoretical consideration of Janus particles actively driving the self-stratification at the coating surfaces.

Janus particles have been tested as coating materials in previous studies.[31–33] However, most studies involve complex synthetic routes such as surface ATRP (atom transfer radical polymerization) to fabricate the Janus particles, which significantly hinders their large-scale industrial applications.[34–36] In addition, the substrate is usually pre-treated with special chemistries or coating layers, such as epoxy groups, to enable the adhesion and precise control of the assembly and orientation of Janus particles. The final coating film structures and properties are also very sensitive to the experimental conditions. The requirement of special substrate and stringent processing conditions almost completely negate the possibility of broad and practical implementation in coating applications. Furthermore, to coat large surface areas, an immense number of Janus particles are needed, which becomes very costly.

Results and discussion

We developed a scalable new hydrophobic coating system comprised of two major components: conventional binder polymer particles and amphiphilic Janus particles. A unique feature of such coating is that Janus particles will self-stratify to the surface and render the coating layer hydrophobic. The experimental evidence for the self-stratification is presented first. Then the dynamics of stratification is studied. Although exhausting all the conditions that can lead to self-stratification is out of the scope of this communication, several parameters that can impact the stratification have been investigated, including pH, binder particle surface charge, particle concentration and Janus particle morphology. A hypothesis and calculation based on a preliminary model are then given to explain the observation, followed by the coating performance comparison between the Janus particles and the homogeneous particles.

First, a scalable and economical synthetic route is established to produce a large quantity of amphiphilic Janus particles based on emulsion polymerization techniques broadly adopted in the coating industry.[37–39] A schematic plot of the reaction procedure is shown in Fig. S1 (ESI†). Details of the particle fabrication are reported in the Experimental section in the ESI.† Then Janus particles are formulated as a straightforward drop-in additive that can be directly applied to the waterborne latex coating system. This means our method is fully compatible with current commercial products, and only a relatively small quantity of Janus particles are needed to cover the surface and change the surface-related coating properties (Fig. 1a). The bulk materials of the coating film remain intact, which helps maintain the coating performance that is unrelated to surfaces. The advantages are obvious – there is no need to completely redesign the current coating system and manufacturers can quickly adapt the new method by simply adding Janus particles in their product lines.

We tested the self-stratification of Janus particles with both the binder particles synthesized in our lab and a commercial primer. Both experiments demonstrated clear stratification of Janus particles at the coating surface. Our binder particles were homogeneous polystyrene particles functionalized with phosphate functional groups through co-polymerization (Fig. S2, ESI†). Phosphate is a known adhesion promoter and the binder

 This journal is © The Royal Society of Chemistry 2020

Open Access Article. Published on 15 June 2020. Downloaded on 7/23/2025 4:24:04 PM.
This article is licensed under a Creative Commons Attribution-NonCommercial 3.0 Unported Licence.

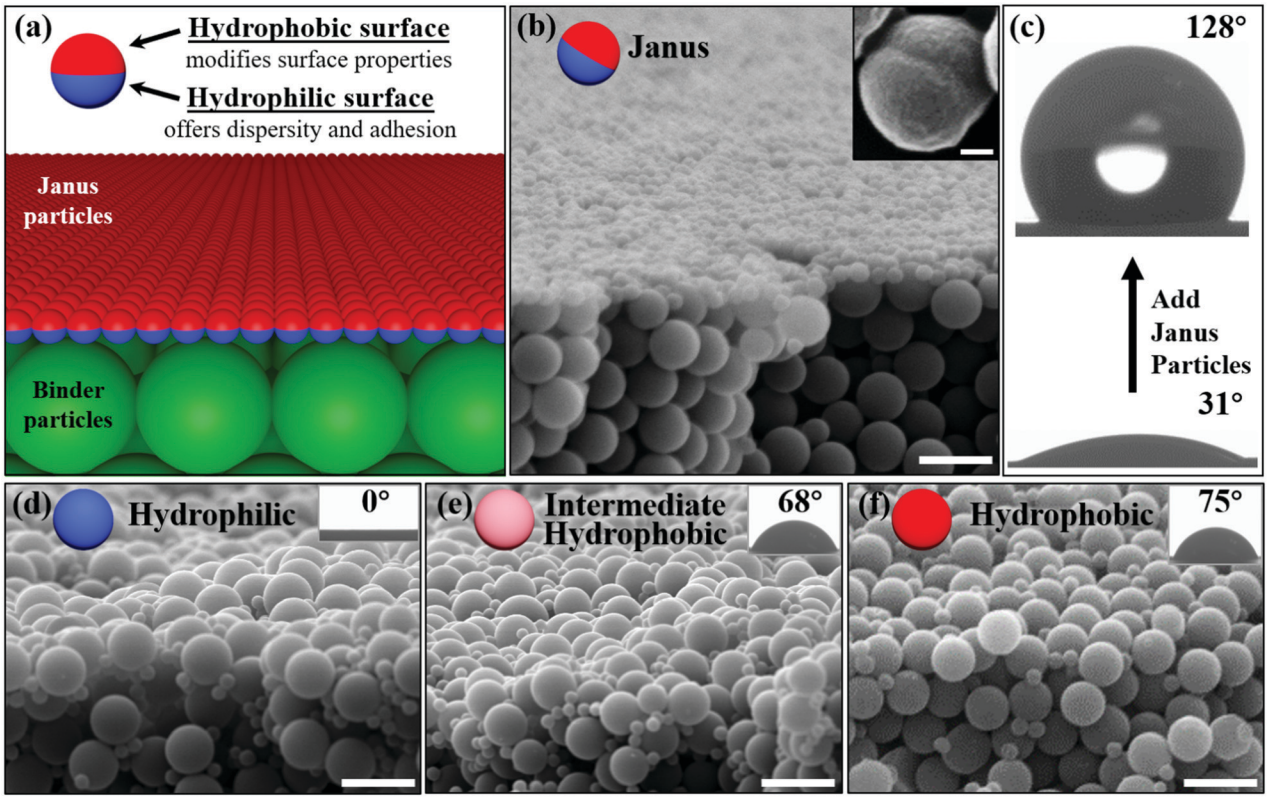

Fig. 1 (a) Schematic diagram for the coating structures formed by self-stratification of amphiphilic Janus particles mixed with binder particles; (b) SEM image of the cross-section view of dried coating structures. Scale bar is 2 μm. Inset shows the asymmetric morphology of a typical Janus particle with Janus balance (percentage of hydrophobic surface area) ~50%. Scale bar is 100 nm; (c) contact angles of the coating surface before and after adding the Janus particles; (d–f) SEM images of the cross-section view of coating films added with homogeneous particles of different amphiphilicity: (d) homogeneous hydrophilic particles; (e) homogeneous intermediate hydrophobic particles; (f) homogeneous hydrophobic particles. Insets show the corresponding contact angles of the coating surfaces. Scale bars are all 2 μm.

particles were designed to provide strong adhesion performance.[40] In a typical experiment, a small number of Janus particles (10% by dry weight) were mixed with binder particles. Ethanol was introduced to help disperse the particles and increase the rate of the evaporation. Fig. 1b shows that a densely packed monolayer of Janus particles self-stratified on top of the homogeneous binder particles. Very few Janus particles were observed in the bulk. In comparison, homogeneous particles of the same size do not migrate to the top surface regardless of the surface hydrophobicity (Fig. 1d–f). In addition, most of the previous studies on stratification with homogeneous particles only show the concentration of stratified particles increases near the surface. It is unique to observe a complete monolayer of particles stratified to the surface. In addition, this densely packed monolayer is the key to drastically improve the water contact angle of the surface.

Due to the weak contrast between two surfaces of polymeric Janus particles under the electron microscope, it is very challenging to directly observe the orientation of Janus particles at the interface. However, the water contact angle of the coating surfaces increased from 31° to 128° after adding Janus particles (Fig. 1c). Since the coating made with pure hydrophobic particles of the same surface chemistry has a contact angle of 131°, the contact angle increase provides the clear evidence that Janus particles orient with their hydrophobic side towards air. In contrast, the contact angles for coating films with homogeneous hydrophilic, intermediate hydrophobic and hydrophobic particles are 0°, 68° and 75° correspondingly, which are much lower than the contact angle of coating film added with Janus particles.

Furthermore, particles with different Janus balance (JB), defined in this paper as the percentage of surface area of the hydrophobic side, also demonstrated different stratification behaviours. Janus particles with low Janus balance (JB equals 20%) did not stratify at all (Fig. S3a, ESI†). Janus particles with bigger hydrophobic patches (JB equals 40%) showed stratification (Fig. S3b, ESI†), however, a small fraction of coating surface was not covered by Janus particles and the stratification is less complete than that of Janus particles with JB of 50% (Fig. 1b). The observation at single particle level correlates very well with the contact angle measurement shown in the insets. These results suggest that adsorption energy, which is determined by the JB, plays an important role in active self-stratification. When adsorption energy is small (JB of 20%), no stratification will occur, while larger adsorption energy (JB of 50%) will lead to the most complete stratification. In addition, Janus particles of 1 μm also showed stratification while homogeneous particles of 1 μm did not show any stratification (Fig. S4, ESI†). This further confirms that Janus geometry is the key to self-stratification.

Open Access Article. Published on 15 June 2020. Downloaded on 7/23/2025 4:24:04 PM.
This article is licensed under a Creative Commons Attribution-NonCommercial 3.0 Unported Licence.

Confocal fluorescent microscopy was utilized to further reveal the kinetics of the active self-stratification process. The amphiphilic Janus particles were labelled with a red fluorescent hydrophobic dye (Nile red) and the hydrophilic binder particles were labelled with a green hydrophilic dye (fluorescein isothiocyanate (FITC)). Larger Janus particles (3 μm) were synthesized to demonstrate the dye labelling and distribution inside Janus particles. Fig. 2a(i) shows the hydrophobic sides of Janus particles were selectively labelled with Nile red. Such fluorescent labelling *via* hydrophobic interaction is highly stable and the dispersity of labelled Janus particles remains unchanged (Fig. 2a(ii)). For contrast, hydrophilic phosphate particles were selectively labelled with hydrophilic FITC (Fig. 2a(iii)) through conjugation. Before the observation, Janus particles and phosphate binder particles were completely mixed under sonication and loaded into a closed chamber. Two different experiments were then carried out to study the kinetics of the self-stratification process. In the open-lid experiment, evaporation was allowed during the observation. In the closed-lid experiment, evaporation was negligible during the observation. The distribution of two types of particles were non-invasively probed using confocal laser scanning microscopy with two excitation wavelengths. It is worth noting that in the open-lid experiment shown in Fig. 2b, amphiphilic Janus particles stratified quickly and exclusively to the top of the solution and formed a thin layer (within 2 minutes). The stratification was completed within just a single confocal scan. Due to the speed limit of confocal scan, the kinetics of the active self-stratification could not be examined in detail. In a closed-lid experiment with negligible evaporation, it was discovered that the self-stratification still happened, albeit slowly (Fig. 2c). The analysis of the confocal scans in the closed-lid experiment reveals that the binder particles remain evenly distributed across the coating suspension. However, Janus particles gradually self-stratified to the top surface within 30 min. The concentration plateau within 5 μm of the top surface is likely due to the resolution limit of the confocal scan. In comparison, when there were no binder particles in the system, Janus particles alone did not self-stratify to the surface in both closed-lid or open-lid experiments (Fig. 2d and e). The observation strongly

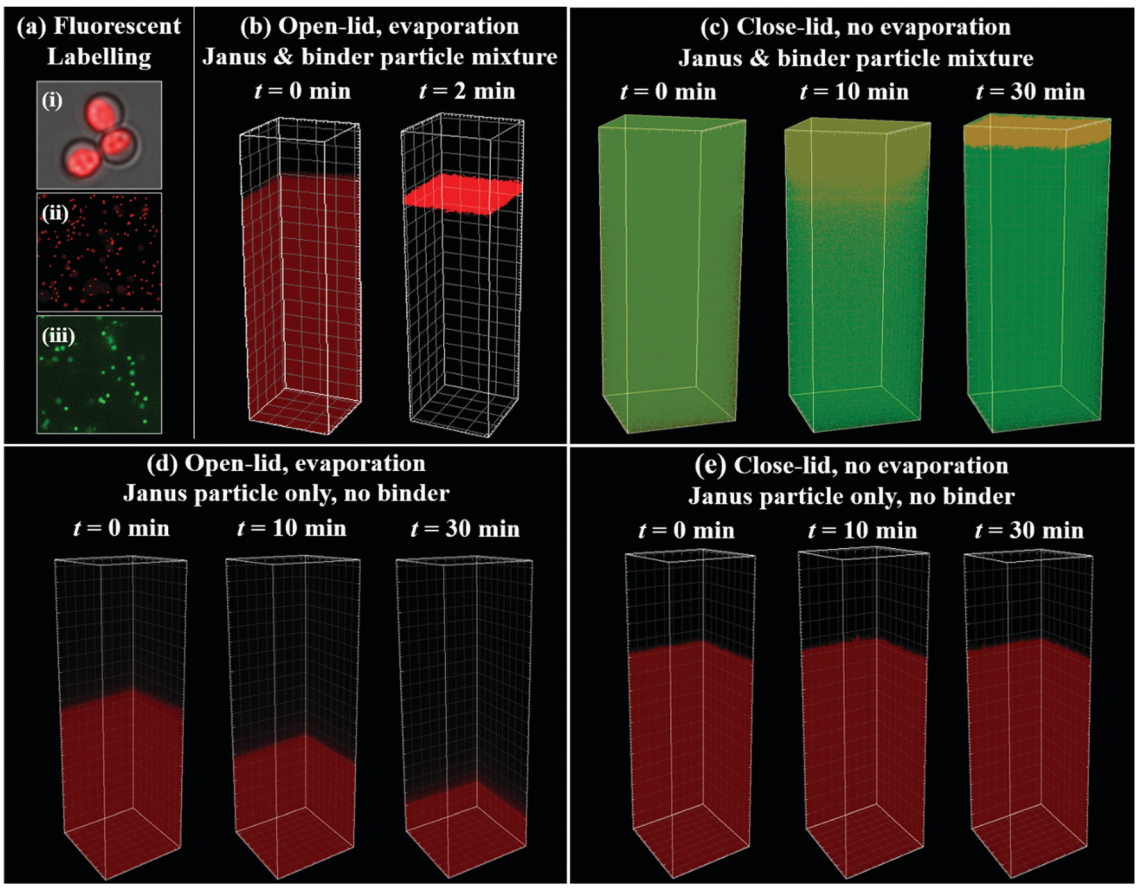

Fig. 2 Fluorescent and confocal microscopy images: (a) fluorescent dye labelled Janus and binder particles: (i) hydrophobic side of 3 μm amphiphilic Janus particles labelled with Nile red; (ii) 400 nm amphiphilic Janus particles labelled with Nile red; (iii) homogeneous 1.3 μm binder particles labelled with green FITC; (b) particle dispersion composed of red amphiphilic Janus particles and unlabelled binder particles at different time points under the evaporation condition (open-lid); (c) particle dispersion composed of red amphiphilic Janus particles and green binder particles at different time points without the evaporation (close-lid); (d) particle dispersion composed of red amphiphilic Janus particles only at different time points under the evaporation condition (open-lid); (e) particle dispersion composed of red amphiphilic Janus particles only at different time points without the evaporation (close-lid).

 This journal is © The Royal Society of Chemistry 2020

Open Access Article. Published on 15 June 2020. Downloaded on 7/23/2025 4:24:04 PM.
This article is licensed under a Creative Commons Attribution-NonCommercial 3.0 Unported Licence.

suggests that interactions between binder particles and Janus particles are critical to the self-stratification.

The active self-stratification of amphiphilic Janus particles is drastically different from previously reported self-stratification of homogeneous particles. This posts a new challenge in developing a suitable model for describing our system. Trueman *et al.* adapted a diffusion model with hydrodynamic interactions to describe stratification in binary colloidal mixtures with different particle sizes.[41] However, this model assumed the chemical potential of the particles was purely entropic and could not predict the accumulation of small particles at the top surface observed in their experiments.[17] Atmuri *et al.* extended this theory to include the interactions between particles of the same species representing the effect of particle surface charge.[42] A term for attraction to the interface (surface adsorption energy) was added to the chemical potential to account for the surface accumulation but no physical basis for this term was given for homogeneous polystyrene particles in that work. Fortini *et al.* proposed an alternative model based on particle migration in an osmotic pressure gradient created by the concentration gradient of particles near the top of the drying film, termed as colloidal diffusiophoresis.[28,43] This model qualitatively predicts that the migration velocity of bigger particles in the osmotic pressure gradient is larger, which results in the small-on-top stratification. The quantitative theory of diffusiophoresis was developed in the framework of dynamical density-functional theory by Zhou *et al.* and Howard *et al.*[29,44,45] Their models identify the cross interaction between large and small particles as the driver for stratification. Hydrodynamic interactions and particle jamming were recently considered in the diffusiophoresis theory but their effects on stratification are still under lively debate.[46–49]

To provide more theoretical support to our observation, we developed a preliminary model that combines the cross interaction between particles and surface adsorption energy, incorporating the surface adsorption energy to account for analysing the active self-stratification of Janus particles. The model adopts the adsorption energy of a particle using characteristic energy scale of the thermal motion at room temperature, which is the product of the Boltzmann constant k_B and the absolute temperature T = 298 K. Theoretical calculation based on an ideal particle estimates the adsorption energy of Janus particles can be several orders of magnitude larger than k_BT.[50,51] However, there is no direct experimental measurement on the adsorption energy of Janus particles used in this work. Many factors including the imperfection of Janus boundary, surface roughness and polymer chemistry are known to influence the adsorption energy. Therefore, the value of 20 k_BT is used as a rough estimation of the minimal value for irreversible adsorption. We also performed the calculation using larger values, which did not change the behaviour of density evolution qualitatively.

Other parameters were taken directly from the experiments, including particle size, concentration ratio, solvent composition, and evaporation rate. Details on the modelling and numerical calculation can be found in the ESI.† The model compares Janus particles with homogeneous particles of the same size when they are both mixed with bigger binder particles and dried under the same conditions. Fig. S5a (ESI†) shows the concentration profiles of different particles across the coating films predicted by the theory at different time points. Initially, Janus particles are evenly distributed throughout the solution and their concentration near the interface is much lower than that of the binder particles (Fig. S6, ESI†). However, Janus particles accumulate rapidly near the interface and their concentration (red line) exceeds the concentration of homogeneous particles (blue line) by two orders of magnitude within 15 min of drying time. Fig. S6 (ESI†) also predicts the depletion of binder particles at the interface driven by the significant concentration gradient of self-stratified Janus particles at the interface. In contrast, the concentrations of both homogeneous and binder particles in their mixtures concurrently increase towards the interface under evaporation with no stratification observed. Notably, this theoretical model is limited to predict the kinetics of active self-stratification at low particle concentrations, therefore unable to capture the progression of stratification through the dense regime towards dense packing. However, the model can be applied to analyse the early stage of stratification when particle concentrations are relatively low. The stratified structure formed at the dilute regime would persist over to higher concentrations, which will subsequently lead to the Janus-on-top structure in the final film.[33]

There are two major assumptions of our preliminary model: (1) interactions between particles are described using a local-density approximation; (2) electrostatic interactions are not considered. Obviously, these assumptions do not fully capture the complexity of the real system and cannot explain why pure Janus particle solution in the absence of binder particles does not exhibit notable surface adsorption (Fig. 2d and e). This suggests that there could be an energy barrier likely due to electrostatic repulsion between the charged particle and the liquid–air surface, which is known to prevent the particles from adsorbing even when the adsorption energy is favourable.[52] However, the preliminary model still provides important insight into particle–particle interactions and particle adsorption at the interface may affect the self-stratification. The discrepancy also suggests that more thorough studies are needed to fully explain the experimental observations.

Commercial coatings are usually formulated at pH $\sim$ 9–11, so binder particle surfaces are rendered with negative charges using acrylic chemistry. Indeed, Janus particles showed the most successful stratification under these conditions as shown in Fig. S7 (ESI†). On the other hand, results in Fig. S7 (ESI†) also indicate many factors may affect the self-stratification, such as pH, binder particle surface charge, and even the concentration of Janus particles. Our study clearly shows that the self-stratification happens when the binder surface is negatively charged, pH is above neutral, Janus particle weight ratio is below 15%, and JB is close to 50%.

Based on these results and preliminary modelling, we provide a tentative hypothesis to explain the unique active self-stratification observations. We hypothesize that due to surface charge of binder particles, they are repelled from the water–air interface and create a depletion zone. Under high particle concentration, the osmotic pressure from the binder particles

Open Access Article. Published on 15 June 2020. Downloaded on 7/23/2025 4:24:04 PM.
This article is licensed under a Creative Commons Attribution-NonCommercial 3.0 Unported Licence.

can drive the accumulation of Janus particles in the depletion zone. In addition, Janus particles are much less charged, which further lowers the barrier of adsorption to the interface. Therefore, we hypothesize that the unique active self-stratification behaviour may be explained by a complex interplay in the following events: (1) depletion of binder particles from the interface due to electrostatic repulsion; (2) accumulation of Janus particles toward the interface due to osmotic pressure from binder particles; (3) the adsorption of Janus particles at the interface due to their amphiphilicity and strong adsorption energy. It is not clear how big the depletion zone would be and whether it can be directly observed in experiment. However, this hypothesis can be used to explain all the experimental observations. Increasing surface charge or pH will increase the repulsion between binder particles and the interface, therefore enlarging the depletion zone and enhancing the osmotic pressure, which increases the possibility for Janus particles to stratify. In Fig. S7 (ESI†), only high surface charge or under pH above neutral, Janus particles with JB close to 50% demonstrated self-stratification.

When Janus particle concentration is higher than their critical micelle concentration, they may self-assemble into clusters, similar to micelles formed by surfactant molecules.[23,53,54] The self-assembled clusters are known to change the kinetics and coating behaviours.[55] The clusters will slow down the diffusion and change the surface adsorption behaviours of Janus particles, which will eventually prevent the stratification from happening. Fig. S7i (ESI†) indeed shows severe aggregation of Janus particles in the bulk when Janus particle concentration is high (30% of the total dry weight).

To investigate the durability of the self-stratified coating surface with Janus particles, organic solvents (EtOH/THF, 90/10 by volume) were used to rinse the surface of the coating films. Coating films formed by mixing homogeneous hydrophobic particles (of the same hydrophobic surface as the Janus particles) and phosphate binder particles were chosen as a control. Images of the cross-sections of the coating films after rinsing in Fig. 3 clearly demonstrate that the self-stratified coating surfaces maintain their structure integrity, and surface hydrophobicity is unchanged. The resistance highlights the completeness of the densely packed monolayer of amphiphilic Janus particles formed during the self-stratification process and the strong adhesion offered by the phosphate binder particles. The hydrophilic binder particles and hydrophilic side of the Janus particles are compatible with each other and may form hydrogen bonds. The compatibility greatly enhances the chance for polymer chains to diffuse and inter-penetrate with each other during the film formation process, which in turn helps promote the strong adhesion between binder particles and Janus particles. In comparison, the control sample that does not possess the stratified structures (Fig. 3b) was destroyed in rinsing with solvent (Fig. 3d). Since the hydrophobic homogeneous particles randomly dispersed within the binder matrix, they acted as the defects and significantly weakened the coating integrity and adhesion. Another interesting observation of the coating films formed by active self-stratification is that these films with Janus particles present a flatter surface compared with the films with only homogenous particles (Fig. S8, ESI†). Previous studies suggest that Janus particles may strongly interact with each other at the interface through capillary attraction and form a strong network. This densely packed network may taper down the fluctuation of the interface.[56]

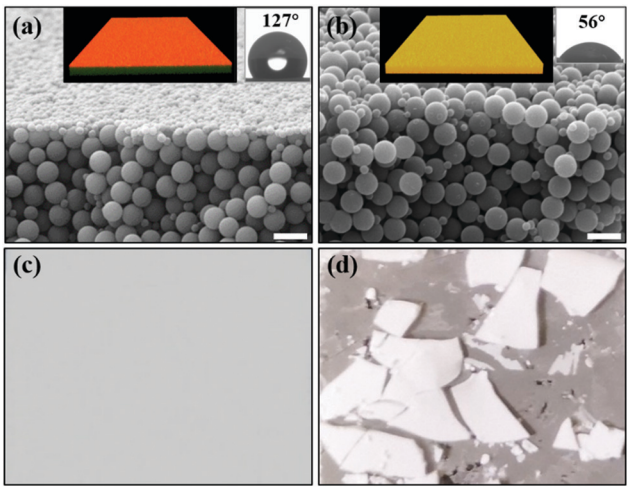

Fig. 3 SEM images and photos of the dried coating films after rinsing with the organic solvent (THF): (a) films formed with Janus particles self-stratified to the surface; (b) films with hydrophobic homogeneous particles showed no stratification. Scale bars are all 2 μm. Insets are confocal fluorescent images of the corresponding coating film and contact angles of coating surface after solvent rinse. Janus and hydrophobic particles were labelled with Nile red and binder particles were labelled with green FITC; (c) photo of the coating film added with Janus particles after solvent rinse; (d) photo of the coating film added with hydrophobic homogeneous particles after solvent rinse.

The self-stratification of Janus particles also offers a novel approach to modulate the nanoscale roughness of the coating surface. It has been well-recognized that higher surface roughness will enhance the water contact angle of hydrophobic surfaces.[57,58] We altered the surface roughness by introducing bigger Janus particles (1 μm) (Fig. S9, ESI†) to co-stratify with smaller Janus nanoparticles (400 nm). Both particles self-stratified to the interface. As shown in Fig. S10 (ESI†), the roughness value measured by confocal microscope is 2.9 μm for coatings made from mixture of 400 nm and 1.0 μm Janus particles, the coating films formed with only 400 nm Janus particles present a flatter surface with a measured roughness of 1.4 μm. Bigger particle size and size mismatch with small particles increased the surface roughness, and a higher water contact angle of 139° (Fig. S11, ESI†) was achieved.

To further test Janus particles with commercial coating products, Janus particles were applied to a common commercial primer. Since commercial coating formulations usually contain many surface-active ingredients beyond simple binder particles, they may interact with Janus particles and interfere with the process. The successful stratification demonstrates the easy integration of our method into existing products. Janus particles (15% by dry weight) was directly added to the commercial primer. The details of the procedure are described in

 This journal is © The Royal Society of Chemistry 2020

Open Access Article. Published on 15 June 2020. Downloaded on 7/23/2025 4:24:04 PM.
This article is licensed under a Creative Commons Attribution-NonCommercial 3.0 Unported Licence.

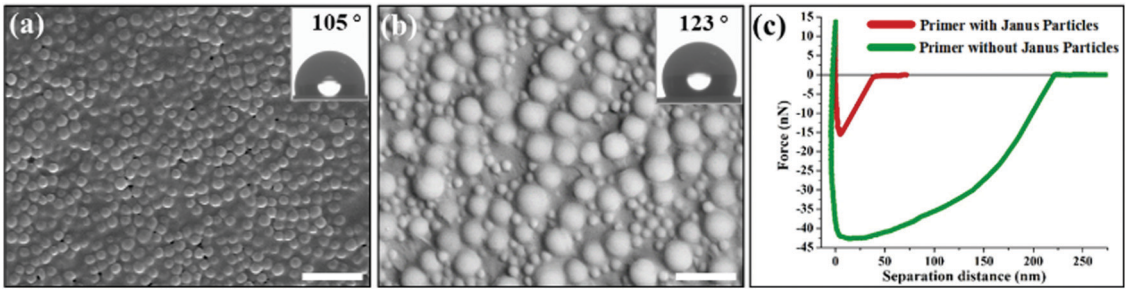

Fig. 4 SEM images of coating films formed by commercial primer binder added with Janus particles, and force profiles measured on film surfaces using AFM: (a) commercial primer added with 400 nm Janus particles; (b) commercial primer added with both 400 nm and 1.0 μm Janus particles; scale bars are all 2 μm. (c) Representative force–distance curves recorded during retraction of AFM tip from the coating film surfaces.

the Experimental section in the ESI.† Fig. 4a clearly shows self-stratification of Janus particles at the surface of the commercial primer coating. Since the primer binder particles have a T_g much lower than the room temperature, they form a continuous film after coating film is dried. Most of the coating surfaces were covered with self-stratified Janus particles and the contact angle was increased from 0° to 105°. Introducing bigger Janus particles to increase roughness further increased the water contact angle to 123° (Fig. 4b). In order to characterize the mechanical properties of the surface, measurement of the surface forces was carried out using AFM (atomic force microscopy). The force–distance curve during retraction of AFM tip from the surface of the primer coating without adding Janus particles in Fig. 4c shows strong adhesion of the top layer (sticky surface). This is expected since the function of the primer is to provide adhesion as a base coat. For the real coating applications, this also means that the primer coating surface is tacky to touch. Without a topcoat, the surface may have poor hardness, stain resistance and dirt pick-up performance. With Janus particles added to the primer formulation, the self-stratified coating showed lower adhesion of top layer, *i.e.* less sticky surface. The average value of rupture force of a tip from the primer surface was reduced to ~1/3 (from 42 nN down to 16 nN) and the range was reduced to ~1/7 (from 210 nm to 30 nm). This demonstrates that Janus particles can not only render the hydrophilic coating film into hydrophobic surface, but also effectively improve the surface properties, such as hardness and tackiness of a commercial product. One advantage of our new approach is that Janus particle additive can be directly applied to coating product without the need to alter the current binder chemistry or coating formulation. The important properties of coating materials, including film formation and dispersion stability, are intact. This method offers a new strategy and more latitude in designing zero-VOC paint with low T_g binder while maintaining the surface properties.

Conclusions

In summary, we demonstrate a new observation of self-stratification using amphiphilic Janus particles. These particles can be produced in large quantity with cost-effective emulsion polymerization. Even better, these amphiphilic Janus particles can be applied directly to current waterborne coating systems as an additive. With a relatively small quantity of Janus particles, they can self-stratify quickly to the surface and form a densely packed monolayer, which creates durable hydrophobic coatings with strong adhesion. The unique fast stratification process and monolayer formation were captured by fluorescent confocal microscopy, which reveals a different physical process compared with the previous self-stratification systems consisting of only homogeneous particles. We determined that the stratification is partially due the strong adsorption of Janus particles at the interface and corroborated this with the preliminary theoretical modelling. Other factors including pH, surface charge of binder particles and particle concentration of Janus particles also contribute to the process. The discovery of active self-stratification provides exciting new opportunities for developing a comprehensive mechanistic understanding of self-stratification of Janus particles. We plan to study the effect of particle size and establish new experimental tools to measure the adsorption energy, which can be used to develop a predictive model in future. The approach demonstrated here is economical and commercially scalable. The successful application of Janus particles in commercial coating products showcases the versatility and effectiveness of our approach and opens a new front for Janus particle research and functionalized coatings. Furthermore, the active self-stratification offers a novel strategy to fabricate hierarchical structures, which may find broad applications in other research areas involving colloidal systems.

Conflicts of interest

There are no conflicts to declare.

Acknowledgements

SJ would like to thank Iowa State University for the Start-up Fund and 3M for the Non-tenured Faculty Award. This work is partially supported by the State of Iowa Biosciences Initiative, American Chemical Society Petroleum Research Fund under Grants No. 60264-DNI7/56884-DNI9 and the Agriculture and Food Research Initiative Grant No. 2019-67013-29016 from the USDA National Institute of Food and Agriculture. We thank Warren Straszheim and Dapeng Jing at the Materials Analysis

Open Access Article. Published on 15 June 2020. Downloaded on 7/23/2025 4:24:04 PM.
This article is licensed under a Creative Commons Attribution-NonCommercial 3.0 Unported Licence.

and Research Laboratory at Iowa State University for helping with the scanning electron microscopy. We also thank Margaret Carter for helping with the confocal microscope at the High Resolution Microscopy Facility of the Iowa State University Office of Biotechnology.

Notes and references

1 S. Jiang, A. Van Dyk, A. Maurice, J. Bohling, D. Fasano and S. Brownell, *Chem. Soc. Rev.*, 2017, **46**, 3792–3807.
2 M. Zubielewicz and A. Królikowska, *Prog. Org. Coat.*, 2009, **66**, 129–136.
3 Y. Joshua Du, M. Damron, G. Tang, H. Zheng, C. J. Chu and J. H. Osborne, *Prog. Org. Coat.*, 2001, **41**, 226–232.
4 W. Zeng, Q. Zhou, H. Zhang and X. Qi, *Dyes Pigm.*, 2018, **151**, 157–164.
5 R. Tejasvi, M. Sharma and K. Upadhyay, *Chem. Eng.*, 2015, **262**, 875–881.
6 G.-m. Wu, Z.-w. Kong, C.-f. Chen, J. Chen, S.-p. Huo and J.-c. Jiang, *J. Appl. Polym. Sci.*, 2013, **128**, 132–138.
7 F. E. Golling, R. Pires, A. Hecking, J. Weikard, F. Richter, K. Danielmeier and D. Dijkstra, *Polym. Int.*, 2019, **68**, 848–855.
8 A. Beaugendre, S. Degoutin, S. Bellayer, C. Pierlot, S. Duquesne, M. Casetta and M. Jimenez, *Prog. Org. Coat.*, 2017, **110**, 210–241.
9 D. J. Walbridge, *Prog. Org. Coat.*, 1996, **28**, 155–159.
10 S. Zahedi, D. Zaarei and S. R. Ghaffarian, *J. Coat. Technol. Res.*, 2018, **15**, 1–12.
11 M. Joo, M. Cakmak and M. D. Soucek, *Prog. Org. Coat.*, 2019, **133**, 145–153.
12 Q. Xie, H. Zeng, Q. Peng, C. Bressy, C. Ma and G. Zhang, *Adv. Mater. Interfaces*, 2019, **6**, 1900535.
13 I. Nikiforow, J. Adams, A. M. König, A. Langhoff, K. Pohl, A. Turshatov and D. Johannsmann, *Langmuir*, 2010, **26**, 13162–13167.
14 Y. Tang, G. S. Grest and S. Cheng, *Langmuir*, 2019, **35**, 4296–4304.
15 A. J. Carr, W. Liu, K. G. Yager, A. F. Routh and S. R. Bhatia, *ACS Appl. Nano Mater.*, 2018, **1**, 4211–4217.
16 I. Martín-Fabiani, A. Fortini, J. Lesage de la Haye, M. L. Koh, S. E. Taylor, E. Bourgeat-Lami, M. Lansalot, F. D'Agosto, R. P. Sear and J. L. Keddie, *ACS Appl. Mater. Interfaces*, 2016, **8**, 34755–34761.
17 R. E. Trueman, E. Lago Domingues, S. N. Emmett, M. W. Murray, J. L. Keddie and A. F. Routh, *Langmuir*, 2012, **28**, 3420–3428.
18 D. K. Makepeace, A. Fortini, A. Markov, P. Locatelli, C. Lindsay, S. Moorhouse, R. Lind, R. P. Sear and J. L. Keddie, *Soft Matter*, 2017, **13**, 6969–6980.
19 N. Glaser, D. J. Adams, A. Böker and G. Krausch, *Langmuir*, 2006, **22**, 5227–5229.
20 A. Kumar, B. J. Park, F. Tu and D. Lee, *Soft Matter*, 2013, **9**, 6604–6617.
21 B. J. Park, T. Brugarolas and D. Lee, *Soft Matter*, 2011, **7**, 6413–6417.
22 S. Jiang, Q. Chen, M. Tripathy, E. Luijten, K. S. Schweizer and S. Granick, *Adv. Mater.*, 2010, **22**, 1060–1071.
23 Q. Chen, J. K. Whitmer, S. Jiang, S. C. Bae, E. Luijten and S. Granick, *Science*, 2011, **331**, 199.
24 S. Jiang and S. Granick, *J. Chem. Phys.*, 2007, **127**, 161102.
25 X. Liu, W. Liu, A. J. Carr, D. Santiago Vazquez, D. Nykypanchuk, P. W. Majewski, A. F. Routh and S. R. Bhatia, *J. Colloid Interface Sci.*, 2018, **515**, 70–77.
26 M. Xiao, Z. Hu, T. E. Gartner, X. Yang, W. Li, A. Jayaraman, N. C. Gianneschi, M. D. Shawkey and A. Dhinojwala, *Sci. Adv.*, 2019, **5**, eaax1254.
27 M. Schulz and J. L. Keddie, *Soft Matter*, 2018, **14**, 6181–6197.
28 A. Fortini, I. Martín-Fabiani, J. L. De La Haye, P.-Y. Dugas, M. Lansalot, F. D'Agosto, E. Bourgeat-Lami, J. L. Keddie and R. P. Sear, *Phys. Rev. Lett.*, 2016, **116**, 118301.
29 J. Zhou, Y. Jiang and M. Doi, *Phys. Rev. Lett.*, 2017, **118**, 108002.
30 X. Wang, X. Feng, G. Ma, L. Yao and M. Ge, *Adv. Mater.*, 2016, **28**, 3131–3137.
31 Z. Cao, Q. Bian, Y. Chen, F. Liang and G. Wang, *ACS Macro Lett.*, 2017, **6**, 1124–1128.
32 J. Zhang, B. A. Grzybowski and S. Granick, *Langmuir*, 2017, **33**, 6964–6977.
33 F. Liang, B. Liu, Z. Cao and Z. Yang, *Langmuir*, 2018, **34**, 4123–4131.
34 S. Berger, L. Ionov and A. Synytska, *Adv. Funct. Mater.*, 2011, **21**, 2338–2344.
35 A. Synytska, R. Khanum, L. Ionov, C. Cherif and C. Bellmann, *ACS Appl. Mater. Interfaces*, 2011, **3**, 1216–1220.
36 H. Yang, F. Liang, Y. Chen, Q. Wang, X. Qu and Z. Yang, *NPG Asia Mater.*, 2015, **7**, e176.
37 Y. Li, S. Chen, S. Demirci, S. Qin, Z. Xu, E. Olson, F. Liu, D. Palm, X. Yong and S. Jiang, *J. Colloid Interface Sci.*, 2019, **543**, 34–42.
38 J. W. Kim, J. Cho, J. Cho, B. J. Park, Y.-J. Kim, K.-H. Choi and J. W. Kim, *Angew. Chem., Int. Ed.*, 2016, **55**, 4509–4513.
39 H. Kim, J. Cho, J. Cho, B. J. Park and J. W. Kim, *ACS Appl. Mater. Interfaces*, 2018, **10**, 1408–1414.
40 N. Rezaee, M. M. Attar and B. Ramezanzadeh, *Surf. Coat. Technol.*, 2013, **236**, 361–367.
41 R. E. Trueman, E. Lago Domingues, S. N. Emmett, M. W. Murray and A. F. Routh, *J. Colloid Interface Sci.*, 2012, **377**, 207–212.
42 A. K. Atmuri, S. R. Bhatia and A. F. Routh, *Langmuir*, 2012, **28**, 2652–2658.
43 A. Fortini and R. P. Sear, *Langmuir*, 2017, **33**, 4796–4805.
44 M. P. Howard, A. Nikoubashman and A. Z. Panagiotopoulos, *Langmuir*, 2017, **33**, 3685–3693.
45 M. P. Howard, A. Nikoubashman and A. Z. Panagiotopoulos, *Langmuir*, 2017, **33**, 11390–11398.
46 R. P. Sear and P. B. Warren, *Phys. Rev. E*, 2017, **96**, 062602.
47 R. P. Sear, *J. Chem. Phys.*, 2018, **148**, 134909.
48 A. Statt, M. P. Howard and A. Z. Panagiotopoulos, *J. Chem. Phys.*, 2018, **149**, 024902.
49 Y. Tang, G. S. Grest and S. Cheng, *J. Chem. Phys.*, 2019, **150**, 224901.
50 B. P. Binks and P. D. I. Fletcher, *Langmuir*, 2001, **17**, 4708–4710.

 This journal is © The Royal Society of Chemistry 2020

Open Access Article. Published on 15 June 2020. Downloaded on 7/23/2025 4:24:04 PM.
This article is licensed under a Creative Commons Attribution-NonCommercial 3.0 Unported Licence.

51 M. A. Fernandez-Rodriguez, M. A. Rodriguez-Valverde, M. A. Cabrerizo-Vilchez and R. Hidalgo-Alvarez, *Adv. Colloid Interface Sci.*, 2016, **233**, 240–254.
52 V. N. Paunov, B. P. Binks and N. P. Ashby, *Langmuir*, 2002, **18**, 6946–6955.
53 A. Tsyrenova, K. Miller, J. Yan, E. Olson, S. M. Anthony and S. Jiang, *Langmuir*, 2019, **35**, 6106–6111.
54 F. Liu, S. Goyal, M. Forrester, T. Ma, K. Miller, Y. Mansoorieh, J. Henjum, L. Zhou, E. Cochran and S. Jiang, *Nano Lett.*, 2019, **19**, 1587–1594.
55 E. Olson, Y. Li, F.-Y. Lin, A. Miller, F. Liu, A. Tsyrenova, D. Palm, G. W. Curtzwiler, K. L. Vorst, E. Cochran and S. Jiang, *ACS Appl. Mater. Interfaces*, 2019, **11**, 24552–24559.
56 K. Miller, A. Tsyrenova, S. M. Anthony, S. Qin, X. Yong and S. Jiang, *Soft Matter*, 2018, **14**, 6793–6798.
57 L. Feng, S. Li, Y. Li, H. Li, L. Zhang, J. Zhai, Y. Song, B. Liu, L. Jiang and D. Zhu, *Adv. Mater.*, 2002, **14**, 1857–1860.
58 M. Liu, S. Wang, Z. Wei, Y. Song and L. Jiang, *Adv. Mater.*, 2009, **21**, 665–669.